Quantum criticality and population trapping of fermions by non-equilibrium lattice modulations

New Journal of Physics
The open access journal for physics

Quantum criticality and population trapping of fermions by non-equilibrium lattice modulations

Regine Frank[1,2]

[1] Institut für Theoretische Festkörperphysik Wolfgang-Gäde-Strasse 1, Karlsruhe Institute of Technology (KIT), D-76131 Karlsruhe, Germany
[2] Institut für Theoretische Physik, Optics and Photonics, Center for Collective Quantum Phenomena (CQ) and Center for Light-Matter Interaction, Sensors and Analytics (LISA+) Eberhard-Karls Universität Tübingen, Auf der Morgenstelle 14, D-72076 Tübingen, Germany
E-mail: r.frank@uni-tuebingen.de

New Journal of Physics **15** (2013) 123030 (13pp)
Received 3 August 2013
Published 17 December 2013
Online at http://www.njp.org/
doi:10.1088/1367-2630/15/12/123030

Abstract. An ultracold gas of interacting fermionic atoms in a three-dimensional optical lattice is considered, where the lattice potential strength is periodically modulated. This non-equilibrium system is non-perturbatively described by means of a Keldysh–Floquet–Green's function approach for Mott–Hubbard systems employing a generalized dynamical mean field theory (DMFT). Strong repulsive interactions between different atoms lead to a Mott insulator state for the equilibrium system, but the additional external driving at zero temperature yields a non-equilibrium quantum critical behavior, where an infinite number of Floquet states arise and a transition to the liquid and conducting phase is given.

Contents

1. Introduction

The melting of crystals and ice has been intriguing ever since Albert Einstein proposed his quantum theory of solids [1]. Novel results in quantum and non-equilibrium physics are pushing us to improve our understanding of how quantum matter behaves at ultra-low temperatures. In condensed matter physics quantum dynamics can only be analyzed under the premise of severe influences due to strong coupling to the environment. This aspect makes it challenging to prepare and control quantum states far from equilibrium. Thus ultracold gases are perfect systems to study the pure influences of quantum non-equilibrium effects in first instance, since the properties of such systems can be tuned almost without restrictions. At this point the reader might ask the question 'Why *non*-equilibrium ?'. Whereas calculations in thermodynamically equilibrated systems are well established in theory, and rather complicated structures requiring high-end numerics can be solved, it is still a challenge to determine results for driven systems [2]. Nevertheless those systems are experimentally and technologically interesting [3–7]. Even if a system is in the steady-state regime, it still does not reside in thermodynamical equilibrium if it is driven, e.g., by a non-zero current or a difference in the potential [8], and the reflection of that fact in theory is highly desirable.

2. Theoretical framework

Recently, intriguing experiments on non-equilibrium dynamics of ultracold gases, both fermionic as well as bosonic, [9–14] have become possible. Among many aspects, also the long time limit of such non-equilibrium systems has been studied [15–17], and applications using non-equilibrium processes as a tool for transport in so called quantum ratchets have been investigated [18].

The Hubbard Hamiltonian is one of the most relevant models for investigating strongly correlated systems in condensed matter theory, of both bosonic as well as fermionic nature [19–23]. In this article we study the characteristics of an interacting ultracold Fermi gas exposed to periodic modulations of the optical lattice strength. This configuration corresponds to a stationary non-equilibrium state, which requires suitable techniques such as the Keldysh formalism. The periodic modulation leads to a 'dressing' of atoms, well known from the application of light fields in quantum optics. We discuss a dynamical mean field theory (DMFT) solution [24] for the Floquet–Keldysh [25] approach. The non-equilibrium-caused dressed states arise as Floquet side bands. In the Mott–Hubbard gap we derive a complicated modulation-induced structure of many particle states, and therefore a transition from the Mott insulting

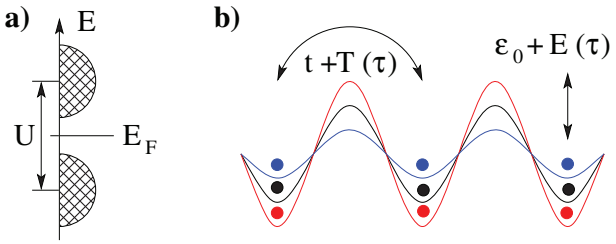

Figure 1. (a) The strong local interaction U between atoms in the equilibrium system causes the single energy band to split into the lower and the upper Hubbard band, separated by an excitation gap. (b) Ultracold fermionic atoms in a three-dimensional optical lattice (black). The optical lattice is periodically modulated with the frequency Ω_{L}, yielding a minimum (red) and a maximum (blue) potential modulation. The periodic modulation introduces an additional, time-dependent contribution to the local atom energy $E(\tau)$ and the atomic tunneling amplitude $T(\tau)$ (see text). The sketched potentials of this non-equilibrium system therefore represent three different snapshots in progress of the external periodic modulation.

regime to a liquid phase which leads to a finite conductivity. The occupation number for these gap states is investigated and we find a trapping of population which results in an 'inversion' for increasing modulation frequencies.

The Fermi gas in the modulated optical potential is schematically shown in figure 1. The Mott insulator state in equilibrium is characterized by a tight binding model with strong repulsive onsite interactions U experimentally determined by a Feshbach resonance. The onsite interaction leads to a band splitting and the establishment of the characteristic Mott–Hubbard gap. Periodic modulations of the optical lattice potential $V(\tau)$ influence the behavior of the tunneling t from one lattice site to the nearest neighbor as well as the onsite energies ϵ_0 at each lattice site. The equilibrium tunneling amplitude t must be replaced by $t + T(\tau)$; the equilibrium onsite energy has to be replaced by $\epsilon_0 + E(\tau)$ as well. These time τ dependent terms are periodic themselves. We consider the following Fermi–Hubbard Hamiltonian:

$$H(\tau) = \sum_{i,\sigma} [\epsilon_0 + E(\tau)]\, c^{\dagger}_{i,\sigma} c_{i,\sigma} - \sum_{\langle ij\rangle,\sigma} [t + T(\tau)]\, c^{\dagger}_{i,\sigma} c_{j,\sigma} + \frac{U}{2} \sum_{i,\sigma} c^{\dagger}_{i,\sigma} c_{i,\sigma} c^{\dagger}_{i,-\sigma} c_{i,-\sigma}. \tag{1}$$

The onsite repulsion U is considered to be not majorly affected by temporal changes, because it is large compared to possible effects due to lattice oscillations. Therefore, U is taken as constant in the following. The index i labels the lattice site and σ the spin; $\langle ij\rangle$ implies summation over nearest neighbors; $c^{\dagger}_{i,\sigma}$ and $c_{i,\sigma}$ create (annihilate) a fermionic atom with spin σ at lattice site i. The time-dependent contributions due to the periodic modulation of the potential are given by

$$E(\tau) = E\cos(\Omega_{\mathrm{L}}\tau) \quad T(\tau) = T\cos(\Omega_{\mathrm{L}}\tau), \tag{2}$$

where Ω_{L} is the frequency of the lattice modulation, τ is the system time and E and T are the respective amplitudes of the energy and the hopping or tunneling contribution. Note, during the numerical evaluation the parameters t and T have to be chosen such that for any time τ the kinetic term in the Hamiltonian, equation (1), does not change sign, i.e. $T(\tau) < t \quad \forall\tau$. The maximum of the hopping amplitude t is set to be equal 8 D, where D is the half bandwidth.

Driven systems, such as fermionic atoms in a modulated lattice potential, experience an energy exchange with their exterior and therefore do not reside in a state of thermodynamical equilibrium. Due to the non-equilibrium character the system response, as e.g. expressed in the Green's function, depends on two distinct time arguments. For instance on a defined starting point and the elapsed time, or after a change of the reference frame on the center-of-mass time and the relative time coordinate. The evolution of an equilibrium state in contrast is usually sufficiently described by the relative time alone. To account for this, Schwinger [26] and in his footsteps Keldysh [27] designed a theoretical framework. The system in the distant past ($\tau = -\infty$) is considered in a defined state, the interaction is then slowly switched on as time progresses, the system evolves to the present where measurements are considered, and then it evolves via ($\tau = +\infty$) back to ($\tau = -\infty$). Along this path the interaction is switched off. This particular time contour is also called Schwinger–Keldysh contour. The time arguments of the Green's function may be found on upper branch of the contour, evolving from $\tau = -\infty$ to $+\infty$ or the time argument may reside on the lower branch, from $\tau = +\infty$ to $-\infty$. A matrix Green's function is considered according to

$$\tilde{\mathbf{G}}(\tau_1, \tau_2) = \begin{pmatrix} G^{++}(\tau_1, \tau_2) & G^{+-}(\tau_1, \tau_2) \\ G^{-+}(\tau_1, \tau_2) & G^{--}(\tau_1, \tau_2) \end{pmatrix} \tag{3}$$

where the superscripts denote on which branch of the contour ($+ =$ upper; $- =$ lower) the respective time arguments τ_1 and τ_2 are found. By a rotation R in the Schwinger–Keldysh space defined by [27]

$$R = \frac{1}{\sqrt{2}} \begin{pmatrix} 1 & 1 \\ -1 & 1 \end{pmatrix}, \tag{4}$$

the matrix Green's function can be rewritten in terms of the more familiar advanced and retarded components of the Green's function according to

$$G(\tau_1, \tau_2) = R^{-1} \tilde{\mathbf{G}}(\tau_1, \tau_2) R = \begin{pmatrix} 0 & G^{\mathrm{A}}(\tau_1, \tau_2) \\ G^{\mathrm{R}}(\tau_1, \tau_2) & G^{\mathrm{Keld}}(\tau_1, \tau_2) \end{pmatrix}, \tag{5}$$

where $G^{\mathrm{Keld}}(\tau_1, \tau_2)$ denotes the Keldysh component of the Schwinger–Keldysh Green's function. The assumed periodic driving of the atomic system encourages the use of the Floquet approach, see e.g. [25]. Then the two-time Green's function requires a generalized two-time Fourier transform according to

$$G^{\alpha\beta}_{m\,n\,;\,\sigma}(\mathbf{k}, \omega, \Omega_{\mathrm{L}}) = \int_{-\infty}^{+\infty} \mathrm{d}\tau_{\mathrm{rel}} \frac{1}{\mathcal{T}} \int_{-\mathcal{T}/2}^{+\mathcal{T}/2} \mathrm{d}\tau_{\mathrm{cm}}\, \mathrm{e}^{\mathrm{i}(\omega - \frac{m+n}{2}\Omega_{\mathrm{L}})\tau_{\mathrm{rel}}} \times \mathrm{e}^{\mathrm{i}(m-n)\Omega_{\mathrm{L}}\tau_{\mathrm{cm}}} G^{\alpha\beta}_{\sigma}(\mathbf{k}, \tau_{\mathrm{rel}}, \tau_{\mathrm{cm}}), \tag{6}$$

where m, n are the Floquet indices labeling the Floquet modes of the system, which are interpreted as the quantized lattice oscillations, the phonons. The system is constrained to absorb and emit energy in multiples of energy quanta $\hbar\Omega_{\mathrm{L}}$. The Keldysh indices are $\alpha, \beta = \pm$, indicating the branch of the Keldysh contour, and $\mathcal{T} = \frac{2\pi}{\Omega_{\mathrm{L}}}$ is the time period. The system-time is shifted to a center-of-motion time $\tau_{\mathrm{cm}} = \frac{\tau_1 + \tau_2}{2}$ and a relative time coordinate $\tau_{\mathrm{rel}} = \tau_1 - \tau_2$. For completeness and later comparison, we note that for the non-interacting case, i.e. $U/D = 0$, the Hamiltonian equation (1) can be solved analytically, yielding

$$G^{R}_{mn}(\mathbf{k}, \omega, \Omega_{\mathrm{L}}) = \sum_{\rho=-\infty}^{\infty} \frac{J_{\rho-m}\left(\frac{E}{\hbar\Omega_{\mathrm{L}}} + T\frac{\tilde{\epsilon}_{\mathbf{k}}}{\hbar\Omega_{\mathrm{L}}}\right) J_{\rho-n}\left(\frac{E}{\hbar\Omega_{\mathrm{L}}} + T\frac{\tilde{\epsilon}_{\mathbf{k}}}{\hbar\Omega_{\mathrm{L}}}\right)}{\hbar\omega - \rho\hbar\Omega_{\mathrm{L}} - \epsilon_{\mathbf{k}} + \mathrm{i}\mathcal{O}}, \tag{7}$$

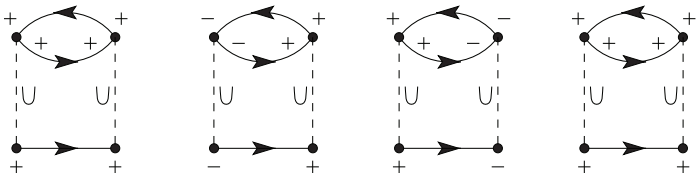

Figure 2. Local self-energy $\Sigma^{\alpha\beta}$ within the iterated perturbation theory (IPT) with its contributing four diagrams. The vertical dashed lines represent the interaction U. The solid lines correspond to the bath-Green's functions, the so-called Weiss-field, $\mathcal{G}^{\alpha\beta}$, cf equation (8). The IPT yields accurate results at half-filling [30].

where we summed over the spins σ, since they are not influenced by the modulation of the potential. In the above equation (7) we introduced Bessel functions $J_{\rho-m}$. We note that $\epsilon_{\mathbf{k}}$ is the dispersion induced by the standard hopping t, i.e. its Fourier transform. Furthermore $\tilde{\epsilon}_{\mathbf{k}}$ originates in the same way from the modulation-induced hopping contribution $T(\tau)$ and is therefore time dependent. Apart from the definition of $\epsilon_{\mathbf{k}}$, we exclude T from the definition $\tilde{\epsilon}_{\mathbf{k}}$. Finally, ρ is the integer summation index.

To solve the full, i.e. driven and interacting system ($U \neq 0$) at zero temperature and half filling, we generalize a DMFT to non-equilibrium. The DMFT [28, 29] maps the interacting lattice system onto a local impurity model embedded in a bath, which consists of all remaining lattice sites in integrated form. The local impurity described by a local lattice Green's function $G^{\alpha\beta}_{mn}(\omega)$ is related to the bath Green's function $\mathcal{G}(\omega)$, the so-called Weiss-field, by the DMFT self-consistency equation. The local self-energy appearing in the local lattice Green's function depends on the Weiss-field, thus closing the self-consistency. The calculation of the self-energy requires further assumption and is achieved by invoking a so-called impurity solver, the iterated perturbation theory (IPT) [30], which is here also generalized to non-equilibrium. The IPT, a diagrammatic method, is demonstrated in figure 2. The DMFT self-consistency equation for the Hamiltonian equation (1) in the above introduced Schwinger–Keldysh–Floquet space is derived as

$$\begin{aligned}\left[\mathcal{G}^{-1}(\omega)\right]^{\alpha\beta}_{mn} = \left[g_0^{-1}(\omega)\right]^{\alpha\beta}_{mn} - \alpha\beta\ \ t\, G^{\alpha\beta}_{mn}(\omega)\ \ t + \alpha\delta_{\alpha\beta}\frac{E}{2}\left[\delta_{m,n+1}+\delta_{m,n-1}+\delta_{m+1,n}+\delta_{m-1,n}\right]\\ + \alpha\beta\left[\frac{T}{2}\left(G^{\alpha\beta}_{m-1,n}(\omega)+G^{\alpha\beta}_{m+1,n}(\omega)\right)t - t\left(G^{\alpha\beta}_{m,n+1}(\omega)+G^{\alpha\beta}_{m,n-1}(\omega)\right)\frac{T}{2}\right]\\ + \alpha\beta\left[\frac{T}{2}\left(G^{\alpha\beta}_{m+1,n+1}(\omega)+G^{\alpha\beta}_{m-1,n-1}(\omega)+G^{\alpha\beta}_{m+1,n-1}(\omega)+G^{\alpha\beta}_{m-1,n+1}(\omega)\right)\frac{T}{2}\right]. \qquad (8)\end{aligned}$$

In the above equation (8) the first line on the rhs compares directly to the equilibrium expression, where the last term in the first line marks the hopping t onto a single site in the lattice and off this single site (often called impurity). Consequently, $\left[g_0^{-1}(\omega)\right]^{\alpha\beta}_{mn} = \alpha\delta_{\alpha\beta}(\omega - n\Omega_{\mathrm{L}})\delta_{nm}$. The second line represents the contribution of the onsite energy modulation originating from the first term on the rhs of the Hamiltonian equation (1), the Kronecker delta symbols have to be interpreted as the different absorption and emission processes of lattice quanta which contribute here. The remaining lines of equation (8), however, represent the part originating from hopping modulations in the driven system. For instance in the third line, processes are found to be characterized by a standard kinetic hopping t on (off) the impurity combined with a phonon

induced hopping T off (on) the impurity. The last line has to be interpreted as the dynamics where both the hopping on and off the impurity are phonon induced. In equation (8) products of the form $\alpha\beta$ assume either the value +1 if $\alpha = \beta$ or -1 otherwise. The DMFT, equation (8) in conjunction with figure 2, offers therefore a solution for a matrix Green's function, which is of the matrix dimension 2×2 in the Schwinger–Keldysh space, cf equation (5) and of the matrix dimension $n \times n$ in the Floquet space. The index n marks the number of involved Floquet side bands in the problem.

3. Results

This substantial numerical effort results in the full knowledge of the non-equilibrium Floquet–Keldysh–Green's function revealing e.g. the local density of states (LDOS), the non-equilibrium distribution function and the relaxation times by means of the self-energy. The assumed initial state is the groundstate of the equilibrium system. From the numerically computed components of the Green's function, we define the LDOS $N(\omega, \Omega_{\mathrm{L}})$ by the following expression, where the momentum is integrated out and Floquet indices are summed:

$$N(\omega, \Omega_{\mathrm{L}}) = -\frac{1}{\pi} \sum_{mn} \int \mathrm{d}^3 k \mathrm{Im}\, G^{\mathrm{R}}_{mn}(\mathbf{k}, \omega, \Omega_{\mathrm{L}}). \tag{9}$$

We define the total non-equilibrium distribution function $F^{\mathrm{neq}}(\omega, \Omega_{\mathrm{L}})$ by the relation

$$\sum_m G^{\mathrm{Keld}}_{0m}(\omega, \Omega_{\mathrm{L}}) = -2\pi \mathrm{i} \left[1 - 2F^{\mathrm{neq}}(\omega, \Omega_{\mathrm{L}})\right] \frac{1}{\pi} \sum_n \mathrm{Im}\, G^{\mathrm{A}}_{0n}(\omega, \Omega_{\mathrm{L}}), \tag{10}$$

resulting in the definition of the total distribution function as

$$F^{\mathrm{neq}}(\omega, \Omega_{\mathrm{L}}) = \frac{1}{2} \left(1 + \frac{1}{2\mathrm{i}} \frac{\sum_m G^{\mathrm{Keld}}_{0m}(\omega, \Omega_{\mathrm{L}})}{\sum_n \mathrm{Im}\, G^{\mathrm{A}}_{0n}(\omega, \Omega_{\mathrm{L}})} \right). \tag{11}$$

A solution for the LDOS, equation (9), is shown in figure 3. There the development of pronounced Floquet side bands in the LDOS structure is discussed. Especially in figure 4 the LDOS for single external frequency but for three different hopping amplitude T is shown. Distinct gap states evolve which induce a transition from the Mott insulator state to the liquid phase. Both features result in severe changes of the fermionic band structure and therefore cause significant changes of, e.g., optical and conduction properties. The behavior of the density of states as a function of the external modulation energy $\hbar\Omega_{\mathrm{L}}$ exhibits two limiting cases with a cross-over regime in between them. For the limit of small modulation frequencies $\hbar\Omega_{\mathrm{L}} \to 0$ it is interesting to note that all Floquet modes gain more and more spectral weight (compare also figure 5). This signals the onset of an orthogonality catastrophe, as predicted by Anderson (AOC) [31]. Anderson states that the ground state of the system is the equilibrium state whereas the zero quasiparticle state does not exist in the fermionic system. The limit of that zero quasiparticle state would correspond to an infinite number of contributing Floquet modes and that state would mark a new ground state which is orthogonal to the original equilibrium state, caused by the change in the potential of the system shown in figure 3. Technically, this is seen as a drastic enhancement of the arguments of the Bessel functions, e.g. for the non-interacting expression in equation (7).

At this point, it should be emphasized that any numerical evaluation is always limited to treatments with a finite number of Floquet modes. Therefore the utilized numerical

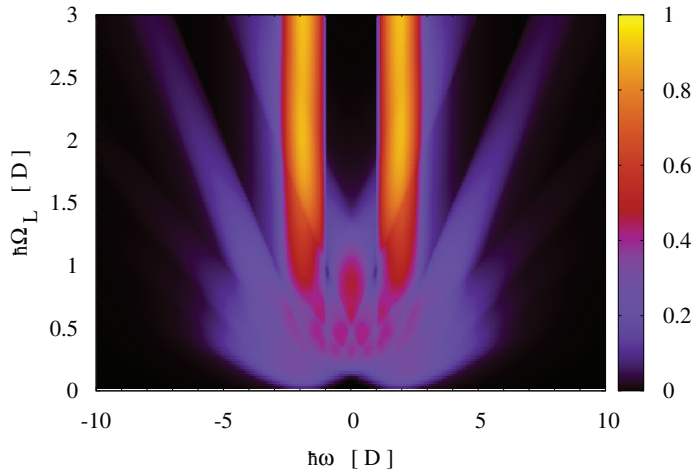

Figure 3. The LDOS $N(\omega, \Omega_L)$, equation (9), as a function of atomic energy $\hbar\omega$ and modulation energy $\hbar\Omega_L$. $T/D = 3.0$, $U/D = 4.0$ and $E/D = 1.0$. The LDOS is displayed as a function of atomic energies $\hbar\omega$ and lattice modulation frequencies $\hbar\Omega_L$. For the limit of $\hbar\Omega_L \to 0$ we find that $N(\omega, \Omega_L)$ is not directly comparable to the equilibrium ground state, but instead a new ground state is reached which features the AOC (see text).

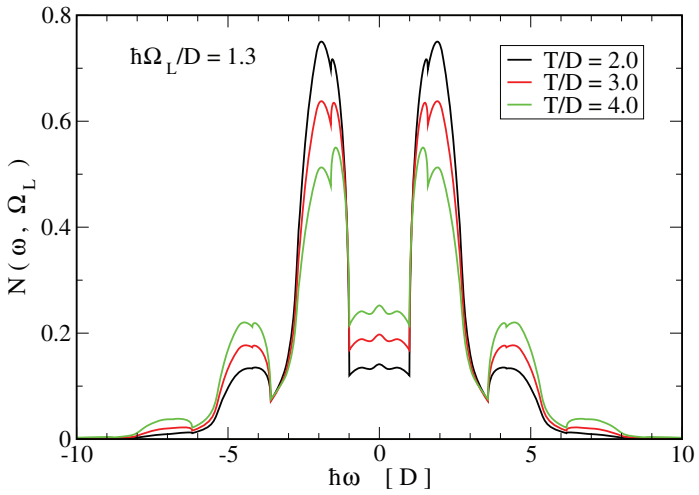

Figure 4. $N(\omega, \Omega_L)$ as a function of atomic energy $\hbar\omega$ and for a single modulation energy $\hbar\Omega_L/D = 1.3$. Displayed are three different hopping strengths $T/D = 2.0, 3.0, 4.0$, other parameters as in figure 3. With increasing hopping the gap states are created and further features are weakened.

implementation is optimized toward the limit of maximum validity at a minimal cost and affordable amount of computational effort. An analysis of the numerical validity in terms of the normalized and frequency integrated density of states

$$N_i(\Omega_L) := \int d\omega N(\omega, \Omega_L) = 1 \tag{12}$$

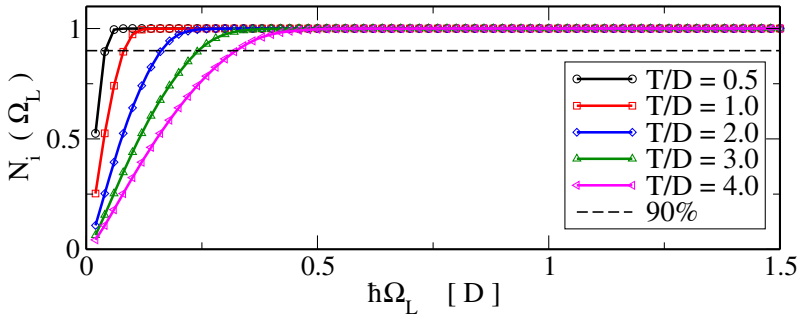

Figure 5. Atomic frequency integrated density of states $N_i(\Omega_L)$, see equation (12), which is normalized to 1. Numerical evaluation for various induced hopping strengths T/D as shown, onsite repulsion strength is $U/D = 4.0$ and $E/D = 1$. The deviations from the value 1 are a measure for the range of validity of the numerics. The dashed horizontal line marks 90% of the norm result, $N_i(\Omega_L)$ above the line indicates a numerical error of less than 10%, considered as valid result.

can be found in figure 5. As a function of the lattice oscillation frequency $\hbar\Omega_L$, the numerical value of the LDOS displays, deviations from its normalization constant 1. The larger the deviation, the larger the encountered numerical error. In figure 5, $N_i(\Omega_L)$ above the horizontal dashed line indicates results with a numerical error of less than 10%, which we will consider valid results here. For increasing hopping strengths T, the numerical accuracy is succeedingly decreased (all other parameters remain unchanged) for small modulation frequencies Ω_L. The physical interpretation of the infinite increase of the number of Floquet–Keldysh–Green's modes contributing for small modulations Ω_L indicate the AOC, see above. Even for the largest considered T, numerical results for modulation energies $\hbar\Omega_L/D > 0.25$ can be considered as accurate within an error range of less than 10% for the used implementation.

In figure 7 we discuss the behavior of the LDOS, equation (9) and the occupation number for increasing external modulation energy $\hbar\Omega_L$. For frequencies $\hbar\Omega_L/D < 1$ the behavior of the ultracold Fermi gas changes from Mott insulating to liquid or conducting. Pronounced Floquet side bands [25] develop and intersect in between the Hubbard bands. The Mott gap almost disappears and a liquid or conducting regime is established, where the liquid density of states can be continuously driven by the external modulation. For the occupation number of the gap states a step-like behavior for long wavelength modulations is found which can be interpreted as the absorption or emission of energy quanta (phonons). In the non-equilibrium fermionic distribution function we derive that for long wavelength modulations the majority of fermions resides in states below the Fermi edge ($\hbar\omega = 0$).

The two limiting regimes of small and large lattice modulations are separated by a cross-over at $\hbar\Omega_L/D \simeq 1$ (see figure 3). At the crossing, the modulation-induced Floquet side bands are forced to intersect (thus crossing) in the gap and acquire a maximum of spectral weight (see figure 6) in this area. Moreover the occupancy from the states right above the lower Hubbard band is shifted towards states right below the upper Hubbard band and additionally the entire gap is almost equally occupied. We further remark that the excitation behavior to reach the upper Hubbard band at the crossing changes from virtual, i.e. successive absorption, to direct.

Right above the crossing, for external modulation frequencies $\hbar\Omega_L/D > 1$, we find that the liquid behavior is dramatically reduced. In the lower panels of figure 7 we discuss the LDOS

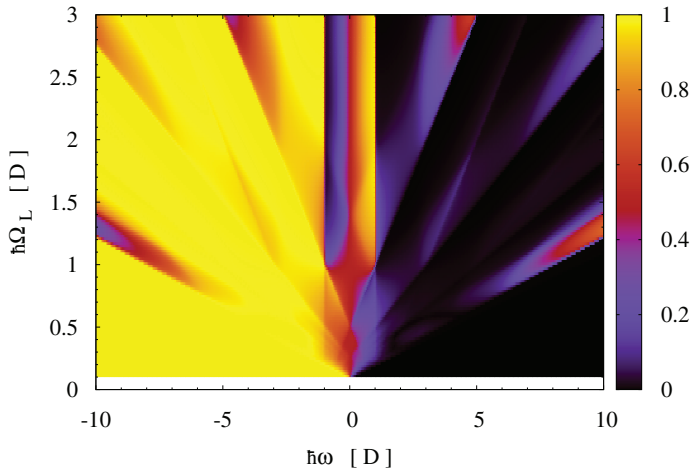

Figure 6. Displayed is the non-equilibrium distribution function $F^{\mathrm{neq}}(\omega, \Omega_{\mathrm{L}})$ in equation (11), as a function of atomic energy $\hbar\omega$ and external modulation energy $\hbar\Omega_{\mathrm{L}}$. The parameters for this original insulating state are $U/D = 4.0$, $T/D = 2.0$, $E/D = 1.0$. Note the behavior around external modulation energies of $\hbar\Omega_{\mathrm{L}}/D \simeq 1$ in the gap region $-1 < \hbar\omega/D < 1$ (see also text).

and the distribution function for external frequencies above $\hbar\Omega_{\mathrm{L}}/D = 1$. Note here that above the crossing the LDOS shows a significant change in the gap. The step-like structure vanishes and exhibits for further increasing modulation energies $\hbar\Omega_{\mathrm{L}}$ almost the behavior of a Mott insulator with an unconventional occupation number in the Mott gap in conjunction with a weak spectral weight there. Combining both, the discussion concerning the spectral weight and the distribution number right above $\hbar\Omega_{\mathrm{L}}/D = 1$, we find a pronounced shift of occupation which resembles a trapping of particles right below the upper Hubbard band, which is an inversion-like situation. This means, atoms occupy energy states above the Fermi energy, especially in the gap region, therefore establishing a population inversion as found and used in other systems to start and maintain lasing behavior. The relaxation of the fermions is impossible because no unoccupied states are within reach for emission processes of an integer number of phonons of the periodic modulation. This effect establishes the atomic population inversion in the pumped system and requests experimental verification. A utilization of the population inversion for other experimental or technological methods might be rather promising, e.g. for phonon pumped lasing. For significantly faster lattice vibrations of the confining potential the system is not able to follow the perturbations and returns to a stationary state similar to equilibrium. The trapping of the occupation is however preserved.

The closing of the Hubbard gap within an intermediate range of the external modulation frequency is also observed by the calculated DC conductivity, which can be written in the form

$$\sigma^{\mathrm{DC}}(\Omega_{\mathrm{L}}) = \lim_{\omega\to 0} \sum_{m} \mathrm{Re}\ \sigma_{0m}(\omega, \Omega_{\mathrm{L}}) \tag{13}$$

$$= \sum_{m} \frac{8e^2t^2}{2\pi^3} \int \mathrm{d}\epsilon N_0(\epsilon) \int \mathrm{d}\omega' \left(\mathrm{Im}\, G^{\mathrm{R}}_{0m}(\epsilon, \omega', \Omega_{\mathrm{L}})\right)^2 \frac{\partial}{\partial\omega'} F^{\mathrm{neq}}_{0m}(\omega', \Omega_{\mathrm{L}}),$$

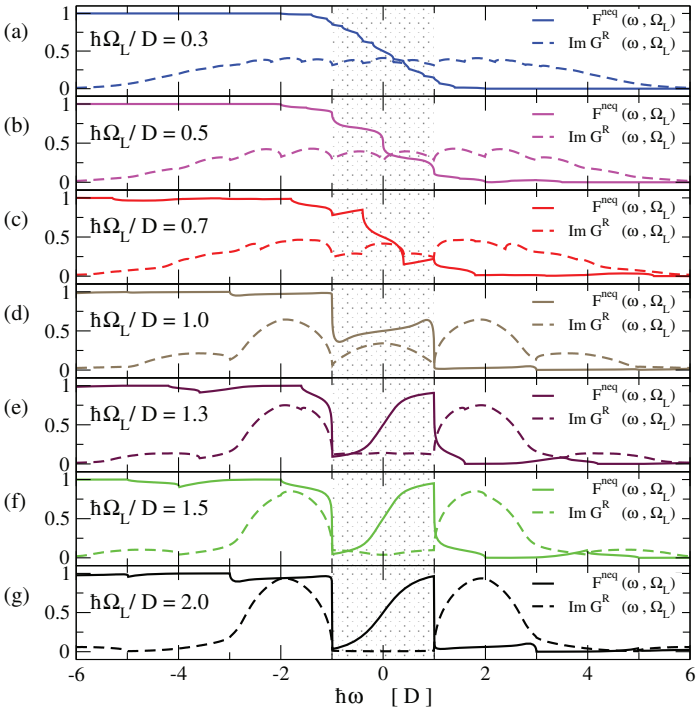

Figure 7. Displayed is $F^{\mathrm{neq}}(\omega, \Omega_{\mathrm{L}})$, equation (11), together with the corresponding LDOS $N(\omega, \Omega_{\mathrm{L}})$, equation (9), for parameters $U/D = 4.0$, $T/D = 2.0$ $E/D = 1.0$ at a series of different external modulation frequencies, $\hbar\Omega_{\mathrm{L}}/D \in \{0.3, 0.5, 0.7, 1.0, 1.3, 1.5, 2.0\}$, from panel (a) to (g). The band gap in equilibrium has the width $2D$, i.e. the hatched region $-1 < \hbar\omega/D < 1$. We note that with increased modulation energies trapping effects of fermions in the Mott gap (hatched area) can be observed. The behavior of the derivative of the distribution function with respect to the frequency ω at the Fermi edge severely influences the conductivity (see figure 8).

where e is the elementary charge, t the hopping amplitude and $N_0(\epsilon)$ is the bare density of states. The non-equilibrium distribution $F^{\mathrm{neq}}_{0m}(\omega, \Omega_{\mathrm{L}})$ is defined by the relation

$$G^{\mathrm{Keld}}_{0m}(\omega, \Omega_{\mathrm{L}}) = -2\pi \mathrm{i}\left[1 - 2F^{\mathrm{neq}}_{0m}(\omega, \Omega_{\mathrm{L}})\right]\frac{1}{\pi}\mathrm{Im}G^{\mathrm{A}}_{0m}(\omega, \Omega_{\mathrm{L}}) \tag{14}$$

$$F^{\mathrm{neq}}_{0m}(\omega, \Omega_{\mathrm{L}}) = \frac{1}{2}\left(1 + \frac{1}{2i}\frac{G^{\mathrm{Keld}}_{0m}(\omega, \Omega_{\mathrm{L}})}{\mathrm{Im}G^{\mathrm{A}}_{0m}(\omega, \Omega_{\mathrm{L}})}\right), \tag{15}$$

where the Keldysh and the advanced component of the Green's function result from the numeric DMFT solution.

The numerical evaluation of the above DC conductivity $\sigma^{\mathrm{DC}}(\Omega_{\mathrm{L}})$, equation (13), is presented in figure 8. The parameters are the same as those given in the caption of figures 5 and 6. We find a strong dependency of $\sigma^{\mathrm{DC}}(\Omega_{\mathrm{L}})$ with respect to the sign changes of the distribution function $F^{\mathrm{neq}}_{0m}(\omega, \Omega_{\mathrm{L}})$. The distinct global maximum in the range $1 \leqslant \hbar\Omega_{\mathrm{L}}/D \leqslant 1.75$ accounts for the intermediate regime, where the absolute height is dominated by the value of the LDOS at the Fermi edge. The somewhat less pronounced peak at larger frequencies

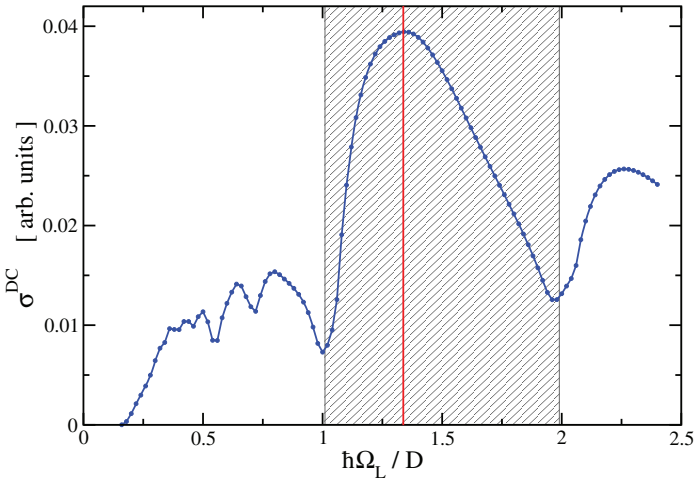

Figure 8. DC conductivity $\sigma^{\mathrm{DC}}(\Omega_{\mathrm{L}})$, equation (13), as a function of external modulation energy $\hbar\Omega_{\mathrm{L}}$. The highest value σ^{DC} corresponds to an external frequency of $\hbar\Omega_{\mathrm{L}}/D \simeq 1.3$ (vertical line). The conductivity not only depends on the absolute value of the LDOS but also on the sign of the derivative of the distribution function $F^{\mathrm{neq}}(\omega, \Omega_{\mathrm{L}})$. Parameters are the same as in figure 7. The hatched area marks the energy region where two-phonon processes excite atoms from the lower to the upper Hubbard band.

$\hbar\Omega_{\mathrm{L}}/D > 2$, however, is also attributed to the strong population inversion in the regime of external lattice modulations. The dominant and lowest in energy process is a two phonon process. Given the width of the gap $\Delta/D = 2$ for $U/D = 4$, an excitation energy of $\hbar\Omega_{\mathrm{L}}/D = 1$ will suffice to bridge the gap and to transfer fermions to the upper Hubbard band. The conductivity in figure 8 also exhibits this behavior. The maximum of $\sigma^{\mathrm{DC}}(\Omega_{\mathrm{L}})$ between $1 < \hbar\Omega_{\mathrm{L}}/D < 2$ reflects just this excitation behavior. Two phonons, each with energy $\hbar\Omega_{\mathrm{L}}/D = 1$, are absorbed by one fermionic atom, therefore the atomic energy is increased by $\hbar\omega/D = 2$, the amount of energy one atom resting at the upper edge of the lower Hubbard band needs to be pumped to a state just above the lower edge of the upper Hubbard band. Consequently, a fermion absorbing two phonons each with energy of $\hbar\Omega_{\mathrm{L}}/D = 2$ raises the atomic energy by $\hbar\omega/D = 4$. A fermion at the lower edge of the lower Hubbard band gaining this amount in energy is transferred to just below the upper edge of the upper Hubbard band. Finally, in figure 8 the form of the conductivity, equation (13), outside the interval $1 < \hbar\Omega_{\mathrm{L}}/D < 2$ is caused by higher Floquet bands involving more than two phonon processes or by excitation dynamics between individual Floquet bands instead of in between the Hubbard bands. The dominant contribution, however, is the lowest excitation in between the two equilibrium Hubbard bands.

4. Conclusion

A theory of ultracold fermionic atoms described by a Hubbard model including strong repulsive interactions is discussed. The quantum criticallity is derived with periodic lattice potential modulations which drive the considered system out of thermodynamical equilibrium. By investigating a Floquet–Keldysh–Green's function approach we find a cross-over at zero

temperature between two limiting characteristics, the AOC for $\hbar\Omega_L/D \to 0$ and a quasi-equilibrium solution for $\hbar\Omega_L/D \to \infty$. Pronounced side-bands lead to a rather complicated density of states in the gap for $\hbar\Omega_L/D < 1$, which indicates a transition to the liquid or conducting regime right at the onset of the modulation. In the vicinity of the cross-over we find a maximum of spectral weight inside the original excitation gap. For external frequencies $\hbar\Omega_L/D > 1$, population trapping in the gap is observed. Beyond, the system approaches an equilibrium-like Mott insulator regime, which indicates that the system is not able to follow fast perturbations.

Acknowledgments

The author thanks A Lubatsch, H Monien and G Schön for stimulating and fruitful discussions. Special thanks go to V Dittrich for reading this manuscript critically. Support by Karlsruhe School of Optics and Photonics (KSOP) is acknowledged. The author is fellow of the Athene program funded by the excellence initiative of the federal government of Germany. We acknowledge support by Deutsche Forschungsgemeinschaft and Open Access Publishing Fund of Karlsruhe Institute of Technology.

References

[1] Coleman P and Schofield A J 2005 Quantum criticality *Nature* **433** 226–9
[2] Trotzky S, Lesanovsky I, Fischer B, Schumm T and Schmiedmayer J 2007 Non-equilibrium coherence dynamics in one-dimensional Bose gases *Nature* **449** 324
[3] Daley A J, Ye J and Zoller P 2011 State-dependent lattices for quantum computing with alkaline-earth-metal atoms *Eur. Phys. J.* D **65** 207
Mark M J, Haller E, Lauber K, Danzl J G, Daley A J and Nägerl H-C 2011 Precision measurements on a tunable Mott insulator of ultracold atoms *Phys. Rev. Lett.* **107** 175301
[4] Tokuno A and Giamarchi T 2011 Spectroscopy for cold atom gases in periodically phase-modulated optical lattices *Phys. Rev. Lett.* **106** 205301
[5] Oka T, Arita R and Aoki H 2003 Breakdown of a mott insulator: a nonadiabatic tunneling mechanism *Phys. Rev. Lett.* **91** 066406
Tsuji N, Oka T and Aoki H 2008 Correlated electron systems periodically driven out of equilibrium: Floquet + DMFT formalism *Phys. Rev.* B **78** 235124
[6] Schneider U *et al* 2012 Fermionic transport and out-of-equilibrium dynamics in a homogeneous Hubbard model with ultracold atoms *Nature Phys.* **8** 213
[7] Bloch I, Dalibard J and Zwerger W 2008 Many-body physics with ultracold gases *Rev. Mod. Phys.* **80** 885
[8] Heidrich-Meisner F, Gonzalez I, Al-Hassanieh K A, Feiguin A E, Rozenberg M J and Dagotto E 2010 Nonequilibrium electronic transport in one-dimensional Mott insulators *Phys. Rev.* B **82** 205110
[9] Schempp H, Günter G, Hofmann C S, Giese C, SalibaS D, DePaola B D, Amthor T, Weidemüller M, Sevincili S and Pohl T 2010 Coherent population trapping with controlled interparticle interactions *Phys. Rev. Lett* **104** 173602
[10] Mullins T *et al* 2009 Photoassociation and coherent transient dynamics in the interaction of ultracold rubidium atoms with shaped femtosecond pulses:I. Experiment *Phys. Rev.* A **80** 063416
[11] Greiner M, Mandel O, Esslinger T, Hänsch T and Bloch I 2002 Quantum phase transition from a superfluid to a Mott insulator in a gas of ultracold atoms *Nature* **415** 39
[12] Sherson J F, Weitenberg C, Endres M, Cheneau M, Bloch I and Kuhr S 2010 Single-atom-resolved fluorescence imaging of an atomic Mott insulator *Nature* **467** 68

[13] Bakr W S, Peng A, Tai M E, Ma R, Simon J, Gillen J I, Fölling S, Pollet L and Greiner M 2010 Probing the superfluid-to-Mott insulator transition at the single-atom level *Science* **329** 547
[14] Greiner M, Regal C A and Jin D S 2005 Probing the excitation spectrum of a Fermi gas in the BCS–BEC crossover regime *Phys. Rev. Lett.* **94** 070403
[15] Kinoshita T, Wenger T and Weiss D S 2006 A quantum Newton's cradle *Nature* **440** 900
[16] Kollath C, Iucci A, McCulloch I P and Giamarchi T 2006 Modulation spectroscopy with ultracold fermions in an optical lattice *Phys. Rev.* A **74** 041604
Kollath C, Iucci A, Giamarchi T, Hofstetter W and Schollwöck U 2006 Spectroscopy of ultracold atoms by periodic lattice modulations *Phys. Rev. Lett.* **97** 050402
[17] Sensarma R, Pekker D, Altman E, Demler E, Strohmaier N, Greif D, Jördens R, Tarruell L, Moritz H and Esslinger T 2010 Lifetime of double occupancies in the Fermi–Hubbard model *Phys. Rev.* B **82** 224302
[18] Salger T, Kling S, Hecking T, Geckeler C, Morales-Molina L and Weitz M 2009 Directed transport of atoms in a Hamiltonian quantum ratchet *Science* **326** 1241
[19] Rigol M, Muramatsu A, Batrouni G G and Scalettar R T 2003 Local quantum criticality in confined Fermions on optical lattices *Phys. Rev. Lett.* **91** 130403
[20] Jaksch D, Bruder C, Cirac J I, Gardiner C W and Zoller P 1998 Cold bosonic atoms in optical lattices *Phys. Rev. Lett.* **81** 3108
[21] Semmler D, Wernsdorfer J, Bissbort U, Byczuk K and Hofstetter W 2010 Localization of correlated fermions in optical lattices with speckle disorder *Phys. Rev.* B **82** 235115
[22] Bruderer M, Johnson T H, Clark S R, Jaksch D, Posazhennikova A and Belzig W 2010 Phonon resonances in atomic currents through Bose–Fermi mixtures in optical lattices *Phys. Rev.* A **82** 043617
[23] Frank R 2013 Population trapping and inversion in ultracold Fermi gases by excitation of the optical lattice—non-equilibrium Floquet–Keldysh description *Appl. Phys.* B **113** 41–7
[24] Freericks J K 2010 Impurity problems for steady-state nonequilibrium dynamical mean-field theory *Physica* E **42** 520–4
[25] Hänggi P 1998 *Quantum Transport and Dissipation Driven Quantum Systems* (New York: Wiley-VCH)
Grifoni M and Hänggi P 1998 Driven quantum tunneling *Phys. Rep.* **304** p 229
[26] Schwinger J 1961 Brownian motion of a quantum oscillator *J. Math. Phys.* **2** 407
[27] Keldysh L V 1965 Diagram technique for nonequilibrium processes *Sov. Phys. JETP* **20** 1018
Landau L D and Lifshitz E M 1981 *Course of Theoretical Physics* vol X (Oxford: Pergamon) chapter 10
[28] Georges A, Kotliar G, Krauth W and Rozenberg M J 1996 Dynamical mean-field theory of strongly correlated fermion systems and the limit of infinite dimensions *Rev. Mod. Phys.* **68** 13
[29] Schmidt P and Monien H 2002 Nonequilibrium dynamical mean-field theory of a strongly correlated system arXiv:cond-mat/0202046
[30] Zhang X Y, Rozenberg M J and Kotliar G 1993 Mott transition in the $d = \infty$ Hubbard model at zero temperature *Phys. Rev. Lett.* **70** 1666
[31] Anderson P W 1967 Infrared catastrophe in Fermi gases with local scattering potentials *Phys. Rev. Lett.* **18** 1049